APPLIED PHYSICS

Nonreciprocal surface acoustic wave propagation via magneto-rotation coupling

Mingran Xu[1,2], Kei Yamamoto[3,2], Jorge Puebla[2]*, Korbinian Baumgaertl[4], Bivas Rana[2], Katsuya Miura[5], Hiromasa Takahashi[5], Dirk Grundler[4,6], Sadamichi Maekawa[2,3,7], Yoshichika Otani[1,2,8]*

A fundamental form of magnon-phonon interaction is an intrinsic property of magnetic materials, the "magneto-elastic coupling." This form of interaction has been the basis for describing magnetostrictive materials and their applications, where strain induces changes of internal magnetic fields. Different from the magnetoelastic coupling, more than 40 years ago, it was proposed that surface acoustic waves may induce surface magnons via rotational motion of the lattice in anisotropic magnets. However, a signature of this magnon-phonon coupling mechanism, termed magneto-rotation coupling, has been elusive. Here, we report the first observation and theoretical framework of the magneto-rotation coupling in a perpendicularly anisotropic film Ta/CoFeB(1.6 nanometers)/MgO, which consequently induces nonreciprocal acoustic wave attenuation with an unprecedented ratio of up to 100% rectification at a theoretically predicted optimized condition. Our work not only experimentally demonstrates a fundamentally new path for investigating magnon-phonon coupling but also justifies the feasibility of the magneto-rotation coupling application.

INTRODUCTION

In a general description, a rectification consists of passing signals in one direction while suppressing those in the opposite direction in a counterpropagation scenario. The best-known example of a rectifier is the electronic diode that converts AC to DC, allowing the development of the huge electronic industry we have today. Despite the great success of the electronic rectifier, challenges remain open, such as efficient rectifiers of small dimensions at high frequencies. Therefore, rectification of other energy entities has been intensively explored, in the form of acoustic rectifiers (*1*, *2*), thermal rectifiers (*3*), magnon rectifiers (*4*), and photon rectifiers (*5*). Here, we demonstrate a giant nonreciprocal behavior of an on-chip acoustomagnetic rectifier at room temperature and gigahertz frequency. Our device exploits the magnon-phonon coupling by which surface acoustic waves (SAWs) interact with ferromagnetic (FM) films and consequently generate spin waves.

At a resonance condition, the coupling of SAWs with magnetic films produces acoustically driven FM resonance (a-FMR) (*6*, *7*). Consequently, the a-FMR generates a spin current that can be converted to charge current by the inverse Edelstein effect (*8*) or spin Hall effect (*9*). Evidence of nonreciprocal behaviors in attenuation of amplitudes was reported when SAWs interacted with magnetic films (*8*, *10*, *11*). In these works, the origin of the nonreciprocal behaviors was attributed to magnetoelastic coupling that induced attenuation, and the interference between the longitudinal and shear components of the strain tensor in SAWs. However, in the thin-film limit, $kd \ll 1$, where $k > 0$ is the absolute value of the wave number of SAWs and d is the film thickness, the shear strain is strongly diminished, and the remaining longitudinal strain is expected to induce only reciprocal magnetization dynamics, ergo limiting the nonreciprocity (NR) that can be achieved. For Rayleigh-type SAWs, there is an additional dynamical component that survives in the thin-film limit, the rotation tensor of elastic deformation, $\omega_{ij} = \frac{1}{2}\left(\frac{\partial u_i}{\partial x_j} - \frac{\partial u_j}{\partial x_i}\right)$, which describes the rotational deformation of the lattice. Here, u_i, $i = x, y, z$ are Cartesian components of the elastic deformation vector field. The nonvanishing ω_{ij} implies that the individual lattice points undergo a rotation per wave cycle, whose chirality changes its sign according to the wave propagation direction (see the blue and red oriented circles in Fig. 1). Furthermore, this rotational term can also couple to the magnetization via magnetic anisotropy, according to the theoretical prediction by Maekawa and Tachiki (*12*).

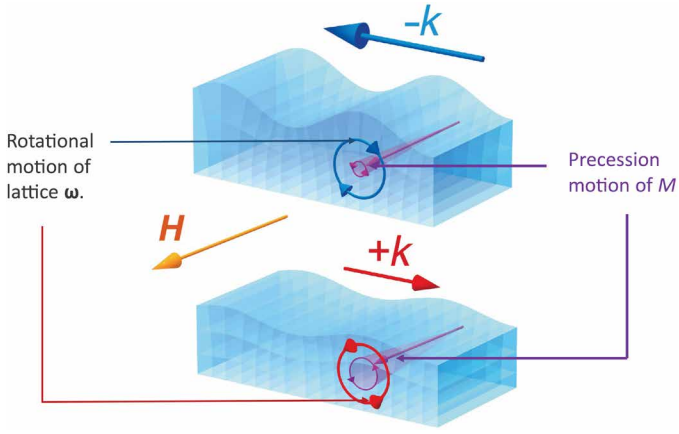

Fig. 1. Schematics of the magneto-rotation coupling. Depending on the propagation direction, SAWs rotate the lattice in opposite directions (as indicted by the blue and red oriented cycles in the figure). This rotational motion couples with the magnetization via magnetic anisotropies, giving rise to a circularly polarized effective field, which either suppresses or enhances the magnetization precession (purple cone), and, in turn, induces a nonreciprocal attenuation on the SAWs.

[1]Institute for Solid State Physics, University of Tokyo, 5-1-5 Kashiwanoha, Kashiwa, Chiba 277-8581, Japan. [2]CEMS, RIKEN, Saitama 351-0198, Japan. [3]Advanced Science Research Center, Japan Atomic Energy Agency, Tokai 319-1195, Japan. [4]Laboratory of Nanoscale Magnetic Materials and Magnonics(LMGN), Institute of Materials (IMX), School of Engineering, Ecole Polytechnique Fédérale de Lausanne (EPFL), 1015 Lausanne, Switzerland. [5]Research and Development Group, Hitachi Ltd., 1-280 Higashi-koigakubo, Kokubunji-shi, Tokyo 185-8601, Japan. [6]Institute of Microengineering (IMT), School of Engineering, Ecole Polytechnique Fédérale de Lausanne (EPFL), 1015 Lausanne, Switzerland. [7]Kavli Institute for Theoretical Sciences, University of Chinese Academy of Sciences, Beijing 100049, People's Republic of China. [8]CREST, Japan Science and Technology Agency, Kawaguchi, Saitama 332-0012, Japan.
*Corresponding author. Email: jorgeluis.pueblanunez@riken.jp (J.P.); yotani@issp.u-tokyo.ac.jp (Y.O.)

Therefore, we extend the previous model taking into account the magneto-rotation coupling, which turns out to be crucial for the giant NR in the present work. The rectification effect that we observe is far larger than the record values of 20% recently reported in (*11*). Our findings go beyond as we theoretically consider the magnetorotation coupling and thereby explain the experimental value of 100% at optimized experimental conditions. This intriguing result is in contrast to (*11*) where it was speculated that the nonreciprocal attenuation depended critically on the magnetic damping.

RESULTS

Figure 2A shows the schematics of SAW propagation through a heterostructure, which consists of four layers, Ta(10 nm)/$Co_{20}Fe_{60}B_{20}$(1.6 nm)/MgO(2 nm)/Al_2O_3(10 nm), on a piezoelectric substrate, *Y*-cut $LiNbO_3$. The acoustic waves are excited by applying a radio frequency (rf) voltage on the input port of interdigital transducers (IDTs), which were patterned by electron beam lithography (EBL). Because of the inverse piezoelectric effect, the rf voltage at a frequency of 6.1 GHz induces vibrations of the lattice, launching SAWs propagating parallel to the *x* axis (see the coordinate system in Fig. 2A). When SAWs propagate through the heterostructure, the oscillation of the lattice points inside the magnet induces an effective rf magnetic field via cubic magnetoelastic coupling and the magneto-rotation coupling. Under a static in-plane external magnetic field $\mathbf{H} = H(\cos\phi, \sin\phi, 0)$, spin waves are excited, which results in SAW attenuation (see Fig. 2B). After passing through the heterostructure, the remaining SAWs are converted back into an rf voltage signal via piezoelectric effect on the output port IDTs. The attenuation was characterized by a vector network analyzer, based on the scattering parameters, S21 and S12. By measuring S21 and S12, we investigated the SAWs propagating along $+x$ and $-x$ direction, respectively, referred to as $+k$ and $-k$ from here on.

Figure 2B shows attenuation spectra for SAW ($+k$) and SAW ($-k$) when an external magnetic field was applied at $\phi = 10^\circ$ in the *xy* plane. The external magnetic field was initially set to 200 mT to saturate the magnetic film and then swept from 120 to 70 mT in 0.5 mT steps. a-FMR is obtained at an external field value of 96 mT, inducing magnetic field–dependent SAW attenuations. However, in the spectra, the SAW ($+k$) shows a negligible attenuation P_{+k}, while SAW ($-k$) shows a relatively large attenuation P_{-k}. The large difference indicates a strong nonreciprocal behavior and, therefore, a strong rectifier effect on acoustic waves. From this, we extract the NR ratio $(P_{+k} - P_{-k})/(P_{+k} + P_{-k})$, which depends on the magnetic field direction, and plot it in Fig. 3. The NR shows a strong dependence on the magnetic field direction with respect to the SAW propagation direction $\hat{\mathbf{x}}$, reaching a maximum value of 100%.

To understand the origin of the giant NR, we theoretically model the magnetization dynamics driven by propagating SAWs in FM thin films. Treating the film as an isotropic elastic body, SAWs propagating along *x* axis are fully characterized by the nonvanishing components ε_{xx}, ε_{xz}, and ε_{zz} of the strain tensor $\varepsilon_{ij} = \frac{1}{2}\left(\frac{\partial u_i}{\partial x_j} + \frac{\partial u_j}{\partial x_i}\right)$ and the rotation ω_{xz}. Among them, the shear strain ε_{xz} scales as kd when the film thickness d is small and becomes negligible compared to the others in our setup where $kd < 10^{-2}$. Thus, the mechanism proposed in (*8*, *10*, *11*) cannot account for the pronounced NR presented above, and another explanation is required. As predicted in (*12*, *13*), a perpendicular magnetic anisotropy, present in our heterostructure, enables the rotation ω_{xz} to generate an effective magnetic field acting on the magnetization. Combined with the conventional magnetoelastic effect that results in an additional effective field proportional to the strain tensor ε_{ij}, the total effective field projected onto the plane perpendicular to the normalized ground-state magnetization $\mathbf{n}$ yields $\mathbf{h} = h_\perp \hat{\mathbf{z}} + h_\parallel \hat{\mathbf{v}}$ where $\hat{\mathbf{v}} = \hat{\mathbf{z}} \times \mathbf{n}$ and

$$h_\perp = \frac{\gamma}{\mu_0 M_s}(2K_u \omega_{xz} - b_2 \varepsilon_{xz})\cos\phi, h_\parallel = \frac{\gamma b_1}{\mu_0 M_s}\varepsilon_{xx}\sin 2\phi \qquad (1)$$

with the cubic magnetoelastic coefficients $b_{1,2}$, the perpendicular uniaxial anisotropy K_u, the gyromagnetic ratio $\gamma < 0$, the saturation magnetization M_s, and the permeability of vacuum μ_0. Further noting that ω_{xz} has exactly the same phase and k dependence as those of ε_{xz}; therefore, we conclude that magneto-rotation coupling is capable of replacing the shear strain as a source of nonreciprocal SAW attenuation. In addition, ω_{xz} is greater by a factor of $(kd)^{-1}$ than ε_{xz} in the thin-film limit so that the resulting NR tends to be much larger when the magnetic anisotropy is comparable to the magnetostriction, which is the case for CoFeB.

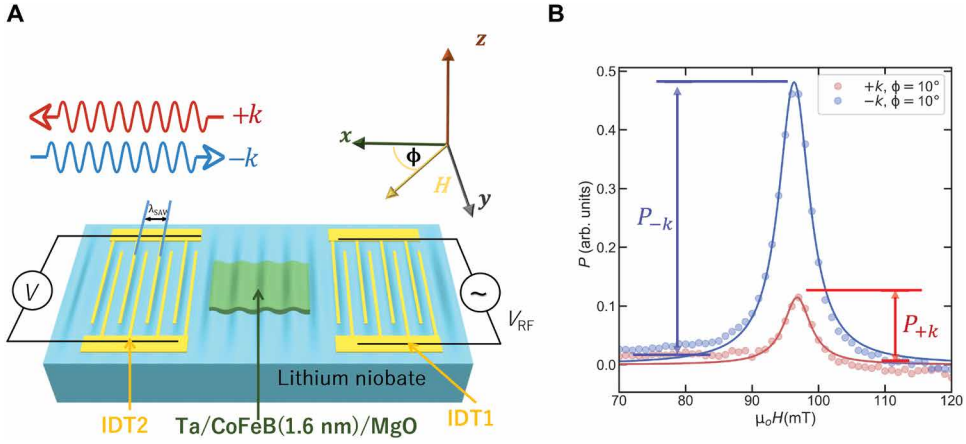

Fig. 2. Nonreciprocal propagation of acoustomagnetic waves in Ta/CoFeB/MgO. (**A**) Device schematics of SAWs coupling to an FM layer at gigahertz frequencies. (**B**) Attenuation of acoustic waves, $P_{\pm k}$, near a spin-wave resonance condition for SAW numbers $+k$ and $-k$. arb. units, arbitrary units.

The SAW attenuation $P_{\pm k}$ is related to the power dissipated by the spin waves excited by the elastic effective field **h**. It can be readily computed as a function of the magnetization angle ϕ, whose details are given in the Supplementary Materials. The formula taking into account of exchange interaction, the uniaxial and cubic magnetic anisotropy, dipole-dipole interaction, and the Dzyaloshinskii-Moriya interaction (DMI) induced by the inversion symmetry breaking at the interface has been used to fit the data in Fig. 3. The agreement is quantitative, suggesting that the magneto-rotation coupling is responsible for the giant NR.

So far, we focused on the nonreciprocal behavior of SAW attenuation $P_{\pm k}$. In addition, we observed a nonreciprocal behavior in the resonance field $H^{res}_{\pm k}$ when the SAW wave number is reversed from k to $-k$. The DMI is the antisymmetric exchange coupling between neighboring magnetic spins, which gives a contribution to the local energy that is linear in spatial derivatives. Therefore, it leads to an asymmetry in spin-wave dispersion relation with respect to the sign of wave number $\pm k$. Commonly, the strength of the DMI or DMI coefficient D is determined by measuring the difference in resonance frequencies between two spin waves propagating in opposite directions (opposite wave numbers, $\pm k$), which is very often achieved by Brillouin light scattering spectroscopy (BLS) (*14*). However, as the magnetic layers become thinner, the magnetic response becomes weaker, which consequently challenges the precise measurement of the DMI coefficient.

With the a-FMR, we observe a clear difference under the resonance condition of the acoustic waves with the spin waves in the 1.6-nm-thick CoFeB layer (see Fig. 4A). After obtaining the resonance field $H^{res}_{\pm k}(\phi)$ as a function of the angle ϕ for $\pm k$ through Lorentzian fits of line shapes (Fig. 4A), we estimate D by fitting the angular dependence of the resonance field difference $\Delta H^{res}(\phi) \equiv H^{res}_{+k}(\phi) - H^{res}_{-k}(\phi)$ by

$$\Delta H^{res}(\phi) = \frac{8D\omega k \sin\phi}{|\gamma|\mu_0^2 M_s \sqrt{(H_v - H_z)^2 + 4(\omega/\gamma\mu_0)^2}} \quad (2)$$

where $H_v - H_z$ depends only on the saturation magnetization, the anisotropy constants, k, and $\cos^2\phi$ (see the Supplementary Materials). As can be seen in Fig. 4B, the observed $\Delta H^{res}(\phi)$ follows the $\sin\phi$ dependence expected for the DMI, yielding $D = 0.089 \pm 0.011$ mJ/m^2, in good agreement with previous reports (*15*) and our BLS characterization (see the Supplementary Materials). This suggests that the acoustic FMR may also serve as an efficient and accurate means of determining the DMI coefficient in magnetic thin films. In addition, for commercial BLS, the maximum wave number k that can be explored is limited by the wavelength of the laser, $k_{max}(\mathrm{BLS}) = \frac{2\pi}{\lambda_{laser}/2} \approx 3 \cdot 10^7$ rad/m, where λ is in the visible range . In contrast, k of the SAW, which is determined by the pitch resolution of EBL, $k_{max}(\mathrm{SAW}) = \frac{2\pi}{4\lambda_{EBL}}$, where $\lambda_{EBL} \approx 10$ nm (*16*), is capable of reaching 10^8 rad/m level. We note that the obtained value of D is too small to account for the NR in the SAW attenuation by the mechanism proposed in (*17*).

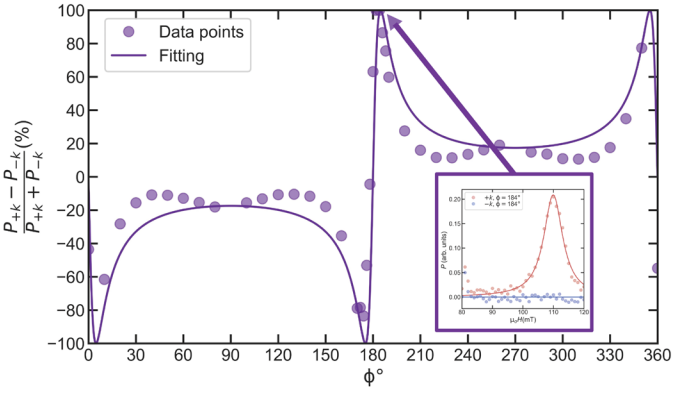

Fig. 3. Dependence of the NR ratio on the magnetic field direction. The magnetic field direction is varied with respect to the SAW propagation direction $\hat{\mathbf{x}}$. We observe a strong variation of the NR ratio, reaching a maximum value of 100% at ϕ = 184°(see the inset).

DISCUSSION

In conclusion, we demonstrated strongly nonreciprocal acoustic attenuation in power (Fig. 2B) and resonance field (Fig. 4A) separately. These intriguing nonreciprocal features of the presented acoustic devices suggest an extraordinary versatility of acoustomagnetic applications. The marked angular dependence of the nonreciprocal

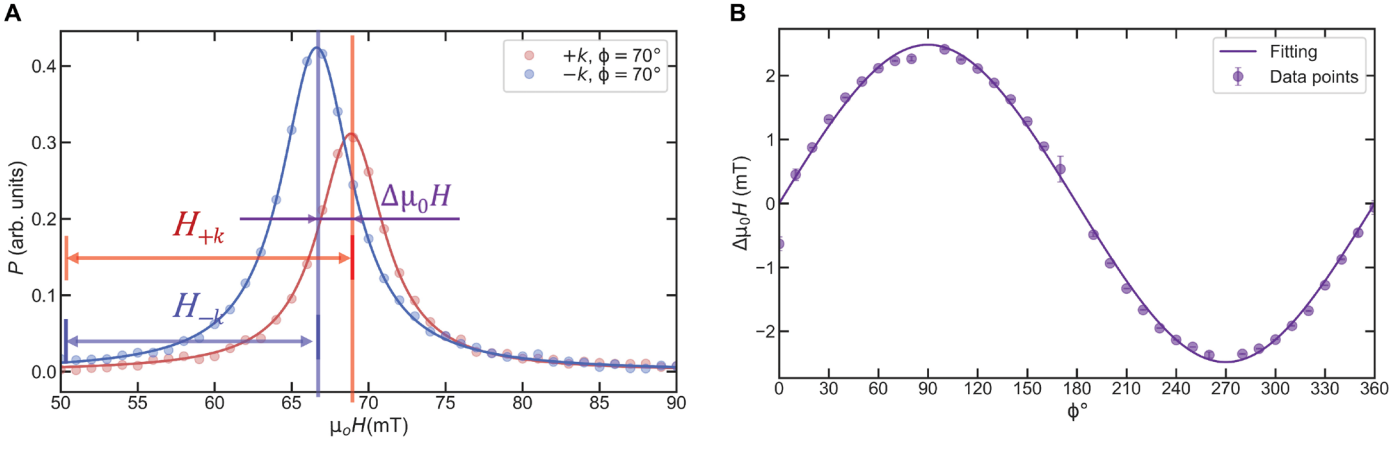

Fig. 4. Assessment of Dzyaloshinskii-Moriya interaction by nonreciprocal magnon-phonon interaction. (**A**) Resonance field difference ΔH_{res} between acoustomagnetic waves was induced by SAWs propagating in $+k$ and $-k$. (**B**) Angle dependence of the resonance field difference between acoustomagnetic waves induced by SAWs with wave numbers $+k$ and $-k$ fitted according to Eq. 2.

ratio (Fig. 3) indicates an efficient and adjustable acoustic rectifier, and the systematic change of NR in resonance field (Fig. 4B) presents its capability as a new route for characterization of DMI. Besides, since the NR introduced here stems from the magnetic anisotropy, it can be further modulated by external electric field, as has been reported for the CoFeB/MgO interface (*18*). Considering the wide application of the general acoustic device in sensing, filtering, and information transportation, utilization of acoustic-magneto rectifier would not only provide highly accurate methods for sensing magnetic properties but also further advance the present acoustic technology and eventually push the development of acoustomagnetic logic devices as an attractive alternative to their magnonic counterparts (*19*, *20*).

MATERIALS AND METHODS

Device fabrication

Figure 2A shows the schematics of SAWs propagation through a heterostructure, which consists of four layers, Ta(10 nm)/$Co_{20}Fe_{60}B_{20}$(1.6 nm)/MgO(2 nm)/Al_2O_3(10 nm), grown by rf sputtering on a piezoelectric substrate, *Y*-cut $LiNbO_3$.

SUPPLEMENTARY MATERIALS

Supplementary material for this article is available at http://advances.sciencemag.org/cgi/content/full/6/32/eabb1724/DC1

REFERENCES AND NOTES

1. X.-F. Li, X. Ni, L. Feng, M.-H. Lu, C. He, Y.-F. Chen, Tunable unidirectional sound propagation through a sonic-crystal-based acoustic diode. *Phys. Rev. Lett.* **106**, 084301 (2011).
2. B. Liang, X. S. Guo, J. Tu, D. Zhang, J. C. Cheng, An acoustic rectifier. *Nat. Mater.* **9**, 989–992 (2010).
3. C. W. Chang, D. Okawa, A. Majumdar, A. Zettl, Solid-state thermal rectifier. *Science* **314**, 1121–1124 (2006).
4. T. Nomura, X.-X. Zhang, S. Zherlitsyn, J. Wosnitza, Y. Tokura, N. Nagaosa, S. Seki, Phonon magnetochiral effect. *Phys. Rev. Lett.* **122**, 145901 (2019).
5. L. Feng, M. Ayache, J. Huang, Y.-L. Xu, M.-H. Lu, Y.-F. Chen, Y. Fainman, A. Scherer, Nonreciprocal light propagation in a silicon photonic circuit. *Science* **333**, 729–733 (2011).
6. M. Weiler, L. Dreher, C. Heeg, H. Huebl, R. Gross, M. S. Brandt, S. T. B. Goennenwein, Elastically driven ferromagnetic resonance in nickel thin films. *Phys. Rev. Lett.* **106**, 117601 (2011).
7. L. Dreher, M. Weiler, M. Pernpeintner, H. Huebl, R. Gross, M. S. Brandt, S. T. B. Goennenwein, Surface acoustic wave driven ferromagnetic resonance in nickel thin films: Theory and experiment. *Phys. Rev. B.* **86**, 134415 (2012).
8. M. Xu, J. Puebla, F. Auvray, B. Rana, K. Kondou, Y. Otani, Inverse Edelstein effect induced by magnon-phonon coupling. *Phys. Rev. B.* **97**, 180301 (2018).
9. M. Weiler, H. Huebl, F. S. Goerg, F. D. Czeschka, R. Gross, S. T. B. Goennenwein, Spin pumping with coherent elastic waves. *Phys. Rev. Lett.* **108**, 176601 (2012).
10. R. Sasaki, Y. Nii, Y. Iguchi, Y. Onose, Nonreciprocal propagation of surface acoustic wave in Ni/$LiNbO_3$. *Phys. Rev. B.* **95**, 020407 (2017).
11. A. Hernández-Mínguez, F. Macià, J. M. Hernàndez, J. Herfort, P. V. Santos, Large non-reciprocal propagation of surface acoustic waves in epitaxial ferromagnetic/semiconductor hybrid structures. *Phys. Rev. Applied* **13**, 044018 (2020).
12. S. Maekawa, M. Tachiki, in *AIP Conference Proceedings* (2008), vol. 29, pp. 542–543.
13. V. G. Bar'yakhtar, V. M. Loktev, S. M. Ryabchenko, Rotational invariance and magnetoflexural oscillations of ferromagnetic plates and rods. *Sov. Phys. JETP.* **61**, 1040–1042 (1985).
14. H. T. Nembach, J. M. Shaw, M. Weiler, E. Jué, T. J. Silva, Linear relation between Heisenberg exchange and interfacial Dzyaloshinskii-Moriya interaction in metal films. *Nat. Phys.* **11**, 825–829 (2015).
15. R. Lo Conte, E. Martinez, A. Hrabec, A. Lamperti, T. Schulz, L. Nasi, L. Lazzarini, R. Mantovan, F. Maccherozzi, S. S. Dhesi, B. Ocker, C. H. Marrows, T. A. Moore, M. Kläui, Role of B diffusion in the interfacial Dzyaloshinskii-Moriya interaction in Ta/Co_{20} Fe_{60} B_{20}/MgO nanowires. *Phys. Rev. B* **91**, 014433 (2015).
16. V. R. Manfrinato, L. Zhang, D. Su, H. Duan, R. G. Hobbs, E. A. Stach, K. K. Berggren, Resolution limits of electron-beam lithography toward the atomic scale. *Nano Lett.* **13**, 1555–1558 (2013).
17. R. Verba, I. Lisenkov, I. Krivorotov, V. Tiberkevich, A. Slavin, Nonreciprocal surface acoustic waves in multilayers with magnetoelastic and interfacial Dzyaloshinskii-Moriya interactions. *Phys. Rev. Appl.* **9**, 064014 (2018).
18. K. Miura, S. Yabuuchi, M. Yamada, M. Ichimura, B. Rana, S. Ogawa, H. Takahashi, Y. Fukuma, Y. Otani, Voltage-induced magnetization dynamics in CoFeB/MgO/CoFeB magnetic tunnel junctions. *Sci. Rep.* **7**, 42511 (2017).
19. B. Rana, Y. C. Otani, Towards magnonic devices based on voltage-controlled magnetic anisotropy. *Commun. Phys.* **2**, 90 (2019).
20. A. Khitun, M. Bao, K. L. Wang, Magnonic logic circuits. *J. Phys. D Appl. Phys.* **43**, 264005 (2010).
21. T. Yu, S. Sharma, Y. M. Blanter, G. E. W. Bauer, Surface dynamics of rough magnetic films. *Phys. Rev. B.* **99**, 174402 (2019).
22. M. Matsuo, J. Ieda, K. Harii, E. Saitoh, S. Maekawa, Mechanical generation of spin current by spin-rotation coupling. *Phys. Rev. B* **87**, 180402 (2013).
23. Z. Tian, D. Sander, J. Kirschner, Nonlinear magnetoelastic coupling of epitaxial layers of Fe, Co, and Ni on Ir(100). *Phys. Rev. B* **79**, 024432 (2009).
24. K. Di, V. L. Zhang, H. S. Lim, S. C. Ng, M. H. Kuok, X. Qiu, H. Yang, Asymmetric spin-wave dispersion due to Dzyaloshinskii-Moriya interaction in an ultrathin Pt/CoFeB film. *Appl. Phys. Lett.* **106**, 052403 (2015).
25. A. K. Chaurasiya, C. Banerjee, S. Pan, S. Sahoo, S. Choudhury, J. Sinha, A. Barman, Direct observation of Interfacial Dzyaloshinskii-Moriya interaction from asymmetric spin-wave propagation in W/CoFeB/SiO_2 heterostructures down to sub-nanometer CoFeB thickness. *Sci. Rep.* **6**, 32592 (2016).
26. B. Rana, Y. Fukuma, K. Miura, H. Takahashi, Y. Otani, Excitation of coherent propagating spin waves in ultrathin CoFeB film by voltage-controlled magnetic anisotropy. *Appl. Phys. Lett.* **111**, 052404 (2017).

Acknowledgments: We would like to thank V. S. Bhat, A. Mucchietto, and S. Watanabe for help in the initial stage of the experiment; O. Gomonay and K. Sato for helpful comments; M. Ishida for her support in preparing figures; Emergent Matter Science Research Support Team in RIKEN for the technical support; and Dongshi Zhang for reviewing the paper. **Funding:** This work was supported by Grants-in-Aid for Scientific Research on Innovative Areas (nos. 26103001 and 26103002) and JSPS KAKENHI (no. 19H05629). M.X. would like to thank support from JSPS through "Research program for Young Scientists" (no. 19 J21720) and RIKEN IPA Program. K.Y. would like to acknowledge support from JSPS KAKENHI (JP 19 K21040) and the Inter-University Cooperative Research Program of the Institute for Materials Research, Tohoku University (proposal no. 19 K0007). S.M. was financially supported by ERATO, Japan Science and Technology Agency (JST), and KAKENHI (nos. 17H02927 and 26103006) from MEXT, Japan. K.B. and D.G. thank SNSF for funding via grant no. 163016. In addition, this work was partially supported by CREST (JPMJCR18T3), JST. **Author contributions:** M.X. and J.P. wrote the main manuscript. M.X. and K.Y. prepared and wrote the Supplementary Materials. M.X. fabricated the samples and performed transmission measurement. K.Y. formulated the theoretical model. M.X. and K.Y. analyzed the data. K.Y. and S.M. developed the explanation of the experimental results. K.B. performed the BLS measurement. K.M. and H.T. grew the CoFeB film. M.X., K.Y, J.P., K.B., B.R., K.M., H.T., D.G., S.M., and Y.O. discussed the results and commented on the manuscript. J.P., S.M., and Y.O. supervised the project. **Competing interests:** The authors declare that they have no competing interests. **Data and materials availability:** All data needed to evaluate the conclusions in the paper are present in the paper and/or the Supplementary Materials. Additional data related to this paper may be requested from the authors.

Submitted 5 February 2020
Accepted 25 June 2020
Published 7 August 2020
10.1126/sciadv.abb1724

Citation: M. Xu, K. Yamamoto, J. Puebla, K. Baumgaertl, B. Rana, K. Miura, H. Takahashi, D. Grundler, S. Maekawa, Y. Otani, Nonreciprocal surface acoustic wave propagation via magneto-rotation coupling. *Sci. Adv.* **6**, eabb1724 (2020).

Science Advances

Nonreciprocal surface acoustic wave propagation via magneto-rotation coupling

Mingran Xu, Kei Yamamoto, Jorge Puebla, Korbinian Baumgaertl, Bivas Rana, Katsuya Miura, Hiromasa Takahashi, Dirk Grundler, Sadamichi Maekawa and Yoshichika Otani

Sci Adv **6** (32), eabb1724.
DOI: 10.1126/sciadv.abb1724